Journal of Cerebral Blood Flow & Metabolism (2015) 35, 565–575

www.jcbfm.com

ORIGINAL ARTICLE

Postsynaptic and spiking activity of pyramidal cells, the principal neurons in the rat hippocampal CA1 region, does not control the resultant BOLD response: a combined electrophysiologic and fMRI approach

Thomas Scherf[1] and Frank Angenstein[1,2]

The specific role of postsynaptic activity for the generation of a functional magnetic resonance imaging (fMRI) response was determined by a simultaneous measurement of generated field excitatory postsynaptic potentials (fEPSPs) and blood oxygen level-dependent (BOLD) response in the rat hippocampal CA1 region during electrical stimulation of the contralateral CA3 region. The stimulation electrode was placed either in the left CA3a/b or CA3c, causing the preferentially basal or apical dendrites of the pyramidal cells in the right CA1 to be activated. Consecutive stimulations with low-intensity stimulation trains (i.e., 16 pulses for 8 seconds) resulted in clear postsynaptic responses of CA1 pyramidal cells, but in no significant BOLD responses. In contrast, consecutive high-intensity stimulation trains resulted in stronger postsynaptic responses that came along with minor (during stimulation of the left CA3a/b) or substantial (during stimulation of the left CA3c) spiking activity of the CA1 pyramidal cells, and resulted in the generation of significant BOLD responses in the left and right hippocampus. Correlating the electrophysiologic parameters of CA1 pyramidal cell activity (fEPSP and spiking activity) with the resultant BOLD response revealed no positive correlation. Consequently, postsynaptic activity of pyramidal cells, the most abundant neurons in the CA1, is not directly linked to the measured BOLD response.

Journal of Cerebral Blood Flow & Metabolism (2015) **35,** 565–575; doi:10.1038/jcbfm.2014.252; published online 7 January 2015

Keywords: CA3; electrophysiology; field excitatory postsynaptic potential; fMRI; hippocampus; neurovascular coupling

INTRODUCTION

Although functional magnetic resonance imaging (fMRI) studies became a widely used tool to study cognitive processes in humans, the underlying neurophysiologic processes are still somewhat enigmatic. In contrast to electroencephalography or magnetoencephalography, fMRI only indirectly visualizes neurophysiologic processes by measuring hemodynamic parameters, such as variations in blood flow, blood volume, or blood oxygenation. Functional magnetic resonance imaging signals are certainly affected by changes in ongoing neuronal activity, but how neuronal activity specifically controls the measured hemodynamic parameters (i.e., neurovascular coupling) is still not entirely clear. Various factors and processes exist that control neurovascular coupling, but to what degree they actually contribute to the measured fMRI signal is often unknown. The most frequently measured hemodynamic parameter for fMRI studies is blood oxygenation. The blood oxygen level-dependent (BOLD) signal depends primarily on the ratio between oxyhemoglobin and deoxyhemoglobin,[1] which in turn is affected by neuronal activity.[2,3] For example, both the activity of principal neurons and interneurons control the BOLD response,[4] but to allocate the exact input of the two different neuron populations for the fMRI response is often uncertain. Similarly, synaptic,[5] spiking activity,[6] and the prevailing intrinsic excitability of the neurons[7] control the BOLD response, but to what extent each of these factors determines the hemodynamic response is not known. Furthermore, the hemodynamic response, the physiologic correlate of the measured fMRI response, may reflect a feedback regulation mechanism (i.e., energy metabolism-related) or a feedforward regulation mechanism (i.e., synaptic (transmitter-release) related).[2] Because of this complexity, a simple approach should be used to study the neurophysiologic basis of fMRI. The authors have previously introduced such an approach that uses monosynaptic activation of dentate gyrus neurons by electrical stimulation of the perforant pathway.[8] Within the dentate gyrus, the generated BOLD response and the spiking activity of principal cells (i.e., granular cells) were simultaneous measured. Consequently, this system focused on the role of principal cell spiking for the generation of the fMRI response in the dentate gyrus. To specifically address the role of postsynaptic activity for the generation of an fMRI response, the hippocampal CA3-CA1 system is now introduced for combined fMRI and electrophysiology measurement. Electrical stimulation of the CA3 causes monosynaptic activation of ipsilateral CA1 pyramidal cells (through

[1]Functional Neuroimaging Group, Deutsches Zentrum für Neurodegenerative Erkrankungen (DZNE), Magdeburg, Germany and [2]Special Lab for Noninvasive Brain Imaging, Leibniz Institute for Neurobiology, Magdeburg, Germany. Correspondence: Dr F Angenstein, Deutsches Zentrum für Neurodegenerative Erkrankungen (DZNE), Leipziger Strasse 44, 39118 Magdeburg, Germany.
E-mail: frank.angenstein@dzne.de or angenstein@lin-magdeburg.de
FA was supported by a grant from the Deutsche Forschungsgemeinschaft (DFG-An200-06).
Received 25 August 2014; accepted 15 December 2014; published online 7 January 2015

Schaffer collaterals) and contralateral CA1 pyramidal cells (through commissural fibers).[9,10] Placing the recording electrode in the *stratum radiatum* of the contralateral CA1 allows the direct measurement of postsynaptic activity of pyramidal CA1 cells, the principal cells in this region. The rising slope of the stimulus-evoked fEPSP is an uncontaminated reflection of the postsynaptic current and is proportional to the amplitude of that postsynaptic current.[11–13] Therefore, the measurement of the initial slope of the field excitatory postsynaptic potential (fEPSP) is suited to relate the amount of postsynaptic activity of principal neurons, i.e., pyramidal cells in the right CA1 region with concurrently generated BOLD response.

Assuming the (post)synaptic activity of principal neurons is the main factor controlling the magnitude of the generated BOLD response, the relation between postsynaptic activity and resultant BOLD response should be similar, irrespective of the mode of spiking. By varying the location of the stimulation electrode in the CA3 region, the activation pathways of contralateral CA1 pyramidal cells can be modified. According to Lorente de Nó, the CA3 region can be divided into three subfields: CA3a, b, and c,[14] with the CA3a subregion distal; the CA3b in the mid part; and the CA3c proximal (close to the dentate gyrus). Stimulation of the left CA3a/b region activates predominantly basal dendrites, whereas stimulation of the left CA3c region activates predominantly apical dendrites of CA1 pyramidal cells.[15,16] As a result, only stimulation of the left CA3c region triggers clear spiking of pyramidal cells, whereas stimulation of the left CA3a/b region only does not (Figure 1). Using these two stimulation conditions, the specific relation between postsynaptic activity and the resultant BOLD response is measured, as well as how additional spiking affects this relation.

MATERIALS AND METHODS

Animals and Surgical Procedure

Animals were cared for and used according to a protocol approved by the animal experiment committee, and in conformity with the European convention for the protection of vertebrate animals used for experimental purposes and institutional guidelines 86/609/CEE, 24 November 1986. The experiments were approved by the animal care committee of the State Saxony-Anhalt, Germany (No. 203h.-42502-2-852-IfN).

For electrode implantation, 9-week-old male Wistar rats ($n = 12$) were anesthetized with Nembutal (40 mg/kg intraperitoneally) and placed in a stereotactic frame. A bipolar stimulation electrode (114 μm in diameter, made from teflon-coated tungsten wire) was either placed in the CA3a/b region at the coordinates AP: − 1.8, ML: − 1.4 mm from Bregma, DV: 2.8 to 3.3 mm from the dural surface ($n = 6$), or into the CA3c region at the coordinates AP: − 2.3, ML: − 1.4 mm from Bregma, DV: 2.9 to 3.5 mm from the dural surface ($n = 6$). A monopolar recording electrode was lowered into the stratum radiatum of the CA1 at the coordinates AP: − 4.0 mm, ML: 2.3 mm from Bregma, DV: 2.1 to 2.6 mm from the dural surface (Figures 1A and 1B). All coordinates for the electrode implantation were taken from the atlas of Paxinos and Watson.[17] The exact locations of the electrodes were histologically verified after completion of the experiments. Monitoring the monosynaptic-evoked field potentials during implantation controlled the correct placement, especially regarding electrode depth. Grounding and indifferent electrodes (silver wires) were set on the dura through the right side of the skull, and fixed in place using acrylic dental cement and plastic screws. The electrodes were additionally attached to a miniature plastic socket and fixed with acrylic dental cement. The wounds were treated with a chlorhexidine containing medical powder. After surgery, animals were provided with ad libitum food and water, and housed individually for a recovery period of 1 week.

Magnetic Resonance Imaging Measurements and CA3 Stimulation

Rats were initially anesthetized with 1.0% to 1.5% isoflurane (in 50:50 N_2: O_2; v:v), and connected to the stimulation and recording electrodes. After placing the animal on the stereotactic platform, narcosis was switched to deep sedation by applying medetomidine (Domitor, Pfizer GmbH, Karlsruhe, Germany), bolus of 50 μg/kg subcutaneously, and after 15 minutes 100 μg/kg per hour subcutaneously.[18] The animals were fixed using a head holder with a bite bar to reduce motion artifacts. Heating was provided from the ventral side (body temperature was measured in some animals before and after the fMRI session and the temperature remained stable between 37.5°C and 38.5°C), breathing rate (between 40 and 60 per minute), heart rate (between 220 and 300 heart beats per minute), and oxygen saturation (between 97% and 99%) were monitored during the whole experiment using an MRI-compatible pulse oxymeter (Mouse Ox, Starr Life Sciences, Pittsburgh, PA, USA). Electrophysiologic responses were evoked by a stimulus generator (Isolated Pulse Stimulator, Model 2100, Science Products, Hofheim, Germany) and recorded with a 5,000-Hz sampling rate and pass filtered from 1 to 5 kHz by using a quad channel differential extracellular amplifier (Ex4-400, Science Products). The signals were transformed by an analog-to-digital interface (power-CED, Cambridge Electronic Design, Cambridge, UK) and stored on a personal computer. Because the switching gradients required for the acquisition of fMR images only generated minor artifacts (Figure 1) no preprocessing of the recorded electrophysiologic data was necessary. For each generated fEPSP, the slope (measured at the steepest rise of the first negative deflection in mV/ms) and the latency were determined (Figures 1C and 1D). To calculate the appropriate stimulation intensities for the fMRI experiment, biphasic constant current pulses (pulse duration 0.2 ms) were applied to the hippocampal CA3 (30 minutes after switching to deep sedation by applying medetomidine) with increasing intensities (i.e., three test pulses at 10-second intervals for the following intensities: 50, 100, 200, 300, 400, and 600 μA) and the evoked CA1 field potentials were recorded. The recordings were taken at 2-minute intervals for lower intensities than 400 μA and 4-minute intervals for all subsequent higher intensities. According to this input/output curve, the intensity required to evoke an fEPSP and the maximal measured slope function could be determined. The correlation between stimulus intensity and measured slope allows for the definition of the two stimulation intensities for the experimental design: a low-stimulation intensity (approximately 50% of the maximal measured slope) without the spiking component in the shape of the fEPSP, and a high-stimulation intensity (approximately 80% of the maximal measured slope) with the spiking component inside the shape of the fEPSP (Figure 1D). Electrical stimulation of the hippocampal CA3, both single test stimuli and burst stimuli, caused no eye or head movements that could perturb the fMRI measurement. Magnetic resonance imaging experiments were performed on a Bruker Biospec 47/20 scanner (Bruker BioSpin GmbH, Ettlingen, Germany) at 4.7T (free bore of 20 cm), equipped with a BGA09 (400 mT/m) gradient system (Bruker BioSpin GmbH, Ettlingen, Germany). A 50-mm Litzcage small animal imaging system (Doty Scientific, Columbia, SC, USA) was used for radio frequency excitation and signal reception. For anatomic images, eight horizontal T_2-weighted spin-echo images were obtained using a rapid acquisition relaxation enhanced sequence,[19] configured using the following parameters: repetition time 4,000 ms, echo time 15 ms, slice thickness 0.8 mm, field of view 37×37 mm, matrix 256×256, rapid acquisition relaxation enhanced factor 8, averages 4. The total scanning time was 8 minutes 32 seconds. Functional MRI was performed using an EPI (echo planar imaging) sequence with the following parameters: repetition time 2,000 ms, echo time 24 ms, slice thickness 0.8 mm, field of view 37×37 mm, matrix 92×92, and total scanning time per frame 2 seconds (Figure 2A).

For the combination of the fMRI and electrophysiologic experiments, the stimulation protocol was divided into three stimulation blocks. Each stimulation block contained 10 stimulation trains with identical stimulus intensities. During the first and third stimulation block, low-intensity pulses were applied. During the second stimulation block, high-intensity pulses were applied. One stimulation train was given every minute (duration of 8 seconds followed by an intertrain interval of 52 seconds) and consisted of 16 pulses with an interpulse interval of 500 ms (i.e., 2 Hz). Trigger pulses that were generated by the scanner at the beginning of every volume, i.e., every 2 seconds, were used to synchronized fMR-image acquisition and electrophysiologic stimulations. The total time for the combined fMRI electrophysiology session was 34 minutes (1,020 frames in fMRI).

Data Processing and Analysis

The functional data were loaded and converted into the BrainVoyager data format. A standard sequence of preprocessing steps implemented in the *BrainVoyager QX* software (Brain Innovation, Maastrich, The Netherlands), such as three-dimensional (3D) motion correction (trilinear interpolation and reduced data using the first volume as a reference) and temporal filtering (high pass (general linear model (GLM)-Fourier): 3 sines/cosines and Gaussian filter, FWHM 3 data points) were applied to each data set.

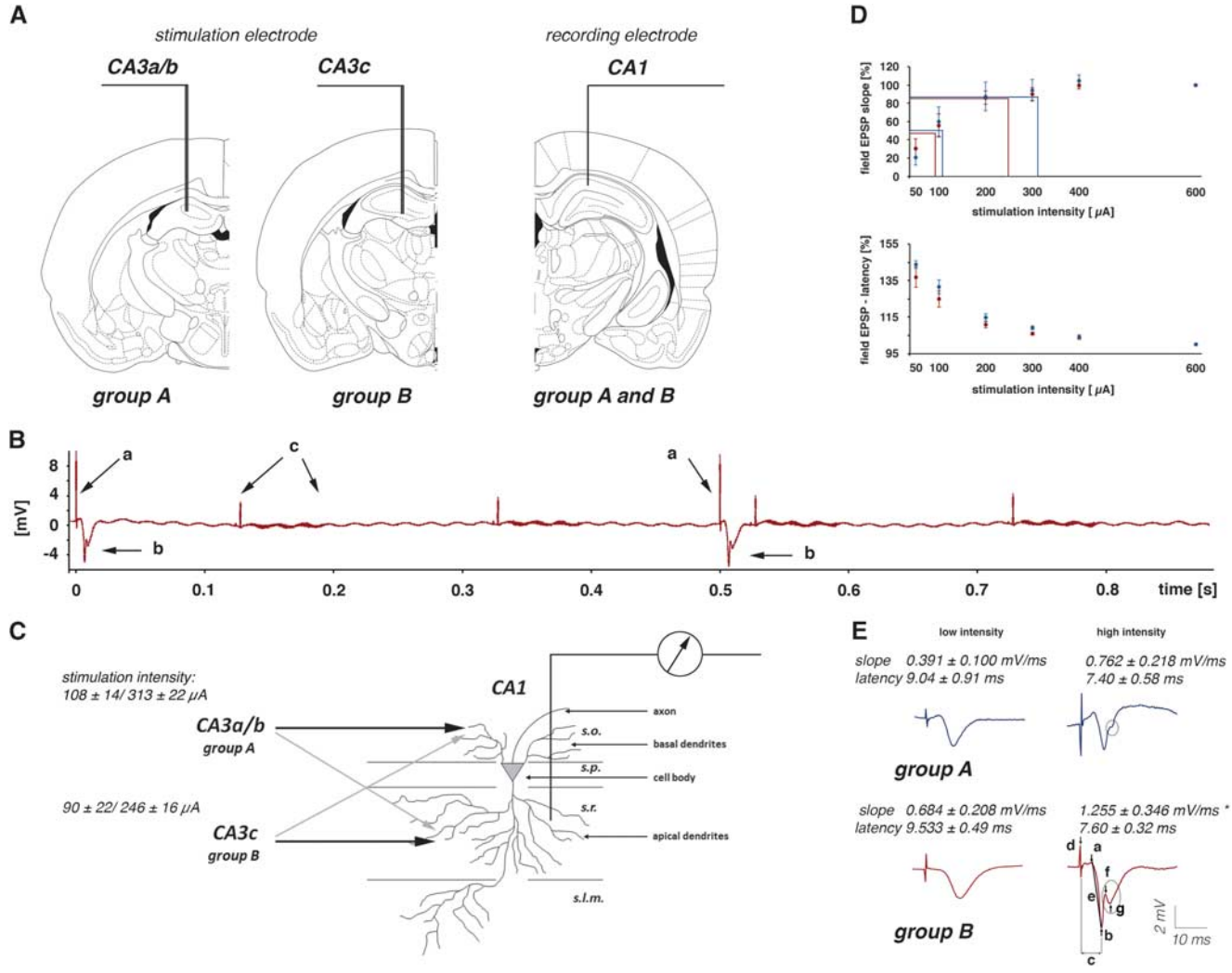

Figure 1. Experimental approach to measure postsynaptic activity during a functional magnetic resonance imaging (fMRI) session. (**A**) One bipolar stimulation electrode was chronically implanted either in the left CA3a/b or in the left CA3c region, and one monopolar recording electrode was placed in the right CA1 region. (**B**) Electrophysiologic recordings during the fMRI measurement. Electrical stimulations of the left CA3 region caused clear detectable stimulation artifacts (a). The response of the pyramidal cells in the right CA1 region appeared after a short latency (b). Switching gradients, required to obtain the fMR images, caused artifacts (c) that were smaller than the field responses generated by the pyramidal cells. Therefore, no additional processing of the electrophysiologic signal was necessary. (**C**) The recording electrode was placed in the stratum radiatum (s.r.); therefore, the recorded field potentials reflect primarily the postsynaptic responses generated in the apical dendrites of CA1 pyramidal cells. Stimulation of pyramidal cells in the left CA3a/b region activates preferentially basal dendrites in the stratum oriens (s.o.), and to a lesser extent, apical dendrites in the stratum radiatum. Stimulation of pyramidal cells in the left CA3c region activates preferentially apical dendrites, and to a lesser extent, basal dendrites of CA1 pyramidal cells. The average stimulation intensities for low- and high-intensity pulses are depicted on the left. (**D**) Summary of the input/output relationship to define the stimulation intensity for low (i.e., 50% of the maximal fEPSP slope) and high (i.e., 80% of the maximal field excitatory postsynaptic potential (fEPSP) slope) intensity pulses. Blue dots represent the input/output curve for animals of group A and red dots represent the input/output curve for animals of group B. (**E**) Recorded field potentials in the right CA1 region during electrical stimulation of the left CA3a/b (group A) and left CA3c (group B). According to the different projections, the average slope as an indicator of the postsynaptic activity in the apical dendrites differs between the two groups. A significant difference in the fEPSP slope between the two groups was found during application of high-intensity stimulation pulses (indicated by an asterisk). In the group B animals, the spike component was consistently detected, whereas in animals of group A, only a deflection was detectable. Parameters to describe the fEPSP: c, latency; d, pulse artifact; e, slope (measured between the markers a and b) and amplitude of the population spike component (measured between the markers f and g).

Because the reconstruction of the fMRI images resulted in a 128×128 matrix (instead of the 92×92 imaging matrix), spatial smoothing (Gaussian filter of 1.4 voxel) was added. Functional activation was analyzed by correlating the observed signal intensity changes in each voxel with the given stimulus protocol using a linear regression analysis (GLM implemented in the *BrainVoyager QX*). Based on this setup, an appropriate activation map was generated. To account for the hemodynamic delay, the stimulus representing block design was modified by a double-gamma hemodynamic response function (HRF) (onset: 0 second; time to response peak: 5 seconds; time to undershoot peak: 15 seconds). To exclude false positive voxels, false discovery rate with a q value of 0.05 (which corresponds to a t value of < 3 or $P < 0.005$) was used as a threshold. For the comparison of region-specific HRF, event-related BOLD responses were calculated by measuring the signal intensities starting at six frames (−12 seconds until 0 second) before stimulus onset (stimulus presentation was between 0 and 8 seconds, which corresponds to 4 frames) until

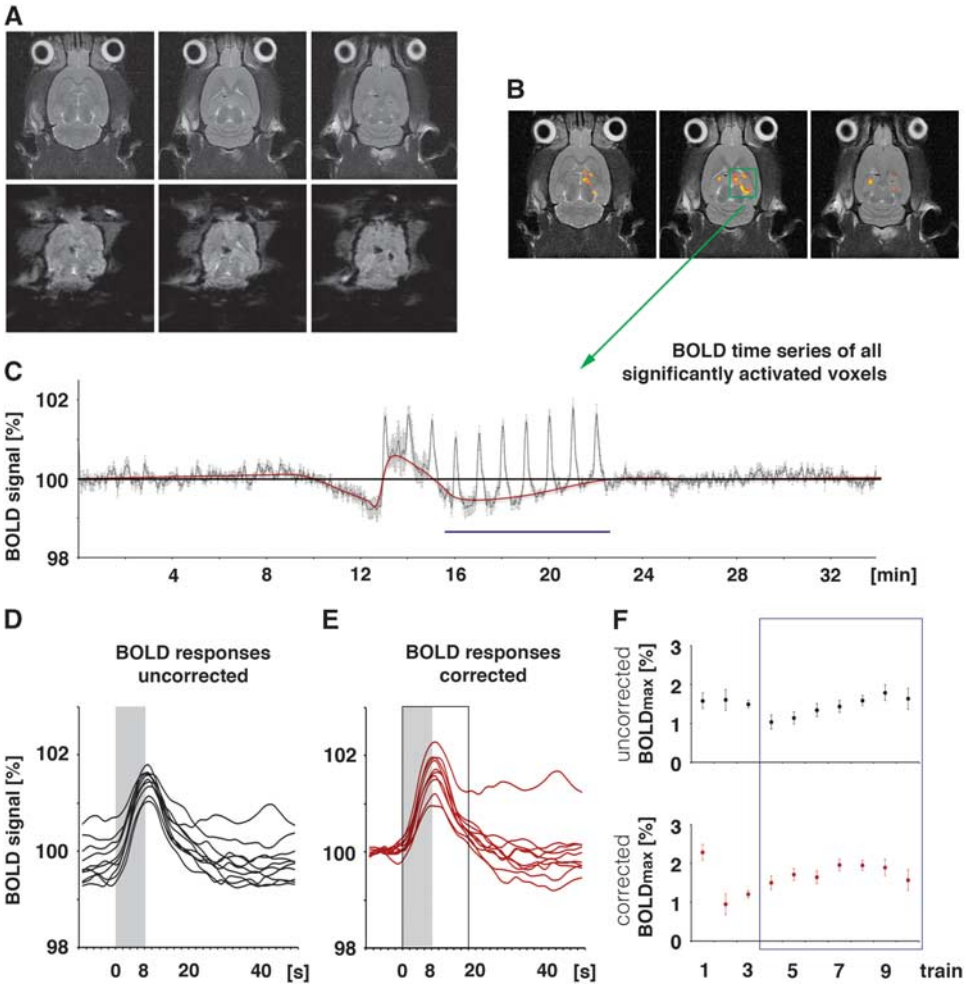

Figure 2. Calculation of the blood oxygen level-dependent (BOLD) response. (**A**) The chronically implanted electrodes caused only minor artifacts in anatomic magnetic resonance (MR) images and small artifacts in the corresponding functional magnetic resonance imaging (fMRI) images. (**B**) A correlation analysis using a general linear model was used to visualize stimulus-related changes in BOLD signal intensities. (**C**) Variations in the BOLD signal intensities were plotted and depicted as BOLD time series. To calculate the maximal BOLD response, the following two approaches were used: (**D**) First, the maximal BOLD response represents the difference between maximal BOLD signal intensity and the average BOLD signal intensity measured during the first 2 minutes of the experiment (indicated by the black line in **C**, i.e., 100%). This approach does not account for putative changes in the baseline BOLD signal intensity. Consequently, individual BOLD responses start at different levels (BOLD responses uncorrected). (**E**) Second, the maximal BOLD response represents the difference between maximal BOLD signal intensity and the actual BOLD signal intensity before application of the stimulus (indicated by a red line in **C**). This approach considers putative variations in baseline BOLD signal intensities. Consequently, individual BOLD responses start at the same level (BOLD responses corrected). Maximal BOLD response is defined as maximal BOLD signal intensity observed between stimulus onset and 10 seconds (or 5 frames) after stimulus cessation (indicated by the black open box). (**F**) When the applied stimulus protocol caused an apparent variation in the baseline BOLD signal intensity, the calculated development of the BOLD responses during consecutive stimulations varied between the two approaches. Because there was a strong variability in the induced BOLD responses during the first three stimulation trains the event-related BOLD was calculated by averaging the individual BOLD responses during trains 4 to 10 (indicated by the blue box in **F** and blue line in **C**).

20 frames (8 to 48 seconds) after the stimulus end. The averaged signal intensities within the appropriate area in the first five frames (−12 seconds until − 2 seconds) were set to 100%. Because there was a high variability of the BOLD responses during the first three stimulation trains only the stimulation trains 4 to 10 were considered for the calculation of the event-related BOLD response. To visualize the activation pattern during each of the three stimulation blocks, all fMRI datasets were aligned to a 3D standard rat brain using anatomic landmarks. These data sets were then analyzed further with a linear regression analysis (GLM multisubject analysis, implemented in the *BrainVoyager QX* software).

Statistical Analysis

All data were reported as group averages ± SEM. For statistical comparison of values among individual experiments, the nonparametric Wilcoxon-signed rank test from the statistical program *WinSTAT* (Ver. 2012.1, R. Fitch Software, Bad Krozingen, Germany) was used. A minimal number of six animals per group were used to perform the Wilcoxon-signed rank test. A paired Student's *t*-test was used to compare BOLD signal intensities within an experimental group. Differences were considered as statistically significant when $P < 0.05$.

RESULTS

As initially determined, electrical stimulation of the two different regions in the left CA3 region generated fEPSPs in the right CA1 region that differed in the size of the population spike component. Stimulating the left CA3a/b region triggered fEPSPs in the right CA1 region with exiguous population spike components, whereas

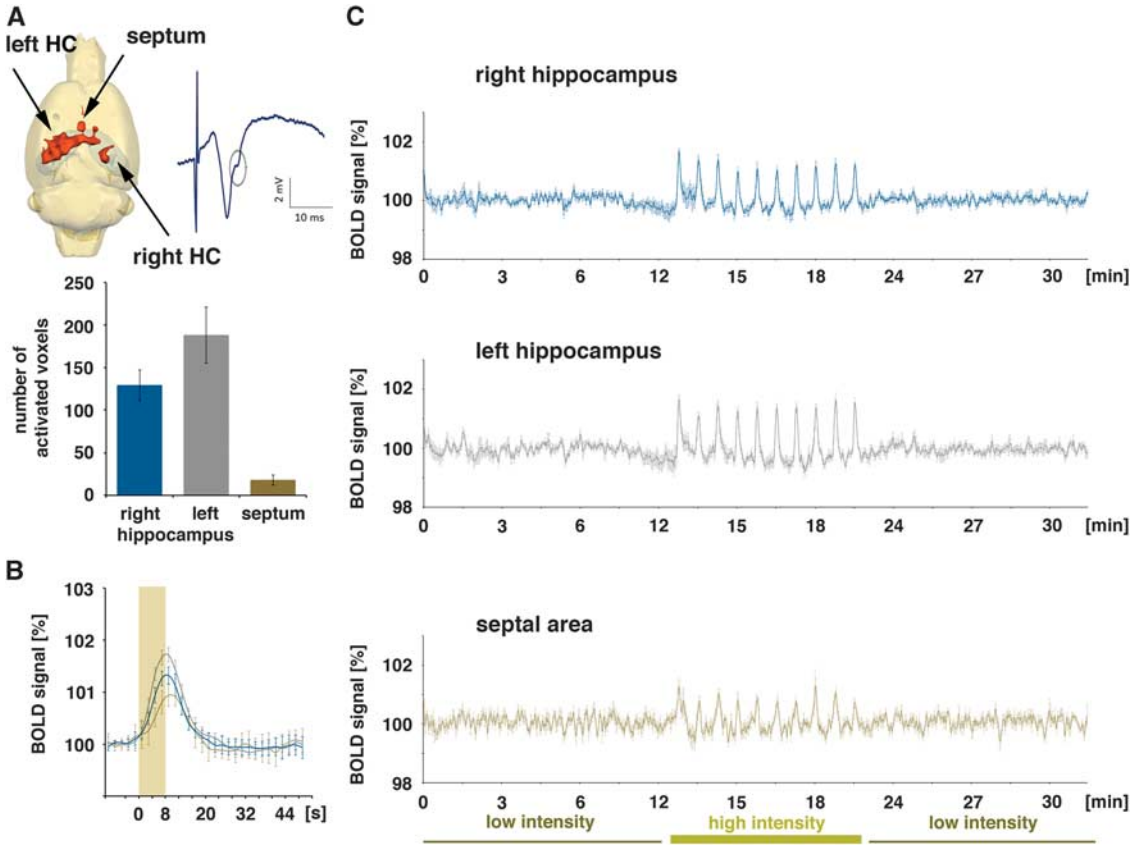

Figure 3. Blood oxygen level-dependent (BOLD) activation pattern generated during repetitive electrical stimulation of the left CA3a/b region (group A, $n = 6$). (**A**) Only during application of high-intensity stimulation pulses were significant BOLD responses observed in the left (stimulated) hippocampus, in the right CA1 region, and in the septal region (an evoked field potential recorded in the right CA1 during stimulation of the left CA3a/b region with one high-intensity stimulation pulse is depicted on the right). Stimulation of the left CA3a/b region resulted in a broadly distributed BOLD response in the left hippocampus and only in a more focused distribution in the right hippocampus (top panel left, quantification in the low panel). (**B**) BOLD responses were generated only during application of high-intensity pulses; the hemodynamic response function was similar in the two hippocampal regions, but different in the septal region (blue line: right hippocampus, gray line: left hippocampus, brown line: septum). (**C**) Entire BOLD time series in the three analyzed regions. During the first and last stimulation block (low-intensity stimulation trains), no stimulus-related variation in BOLD signal intensities was observed, whereas during the second stimulation block (high-intensity stimulation trains), each stimulus train caused a clear BOLD response in all three regions.

stimulation of the left CA3c region triggered fEPSPs in the right CA1 region with strong population spike components (Figure 1E). The two stimulation conditions caused substantial postsynaptic activations in the same right CA1 region. The fEPSPs show this postsynaptic activation was accompanied by minor spiking, yet substantial spiking of pyramidal cells. To address the question of whether postsynaptic activity alone or only the combined postsynaptic and spiking activity controls the magnitude of a BOLD response, the authors compared the generated BOLD response in the right CA1 region during stimulation of the left CA3a/b (Figure 3) or left CA3c (Figure 4) region with low- and high-intensity pulses.

Correlation of the Blood Oxygen Level-Dependent Response and Pyramidal Cell Activity in the Right CA1 Region during Electrical Stimulation of the Left CA3a/b Region

Similar to previous studies, repetitive identical stimulation trains generated different BOLD responses, concurrently with different pyramidal cell activations. In general, low-intensity stimulations of the left CA3 region caused similar electrophysiologic responses in the right CA1 region to all consecutive pulses in one individual train. These substantial postsynaptic activations were not accompanied by any significant changes in BOLD signal intensities—neither in the stimulated left hippocampus nor in the concurrently activated right hippocampus.

Increasing the stimulation intensity caused significantly stronger postsynaptic activations and the appearance of minor deflections in the fEPSPs, indicating minor spiking of CA1 pyramidal cells (Figures 1 and 3). Within each individual train, the 16 consecutive pulses generated slightly decreasing fEPSPs, i.e., the slope of the last fEPSP was significantly smaller than the slope of the first fEPSP (Figure 5), whereas the latency remained similar. In addition, the average synaptic responses varied during consecutive stimulation trains, i.e., the average slope of the fEPSPs increased significantly after the first stimulus train and then remained almost stable during the following nine trains. In contrast to the slope, the latencies of the average fEPSPs remained similar during all consecutive trains (Figure 6). Consequently, consecutive applied pulses within each individual stimulus train, as well as repetitive stimulation trains, caused changes in the signal processing within the right CA1 region.

The high-intensity stimulation protocol induced significant BOLD responses in the stimulated left hippocampus, in the concurrently activated right hippocampus, and in the septal region. Within the hippocampal formation, the stimulation caused

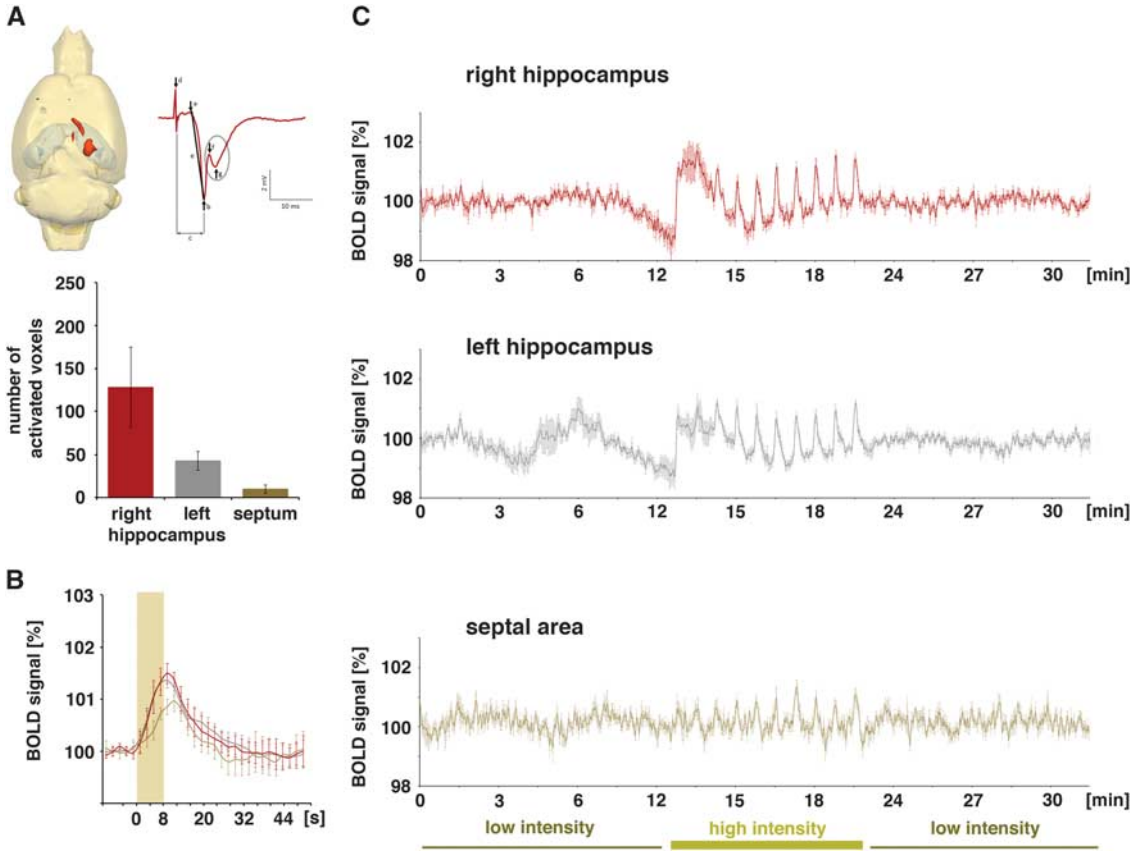

Figure 4. Blood oxygen level-dependent (BOLD) activation pattern generated during repetitive electrical stimulation of the left CA3c region (group B, $n = 6$). (**A**) Significant BOLD responses were observed primarily in the right CA1 region and in the septal region. Significant BOLD responses were only generated during application of high-intensity pulses (evoked field potentials, recorded in the right CA1 during stimulation of the left CA3c region with one high-intensity stimulation pulse, is depicted on the right). Quantification of the number of significantly activated voxels in each region is shown in the lower part. (**B**) Comparison of the hemodynamic response function in each region was similar to group A. (**C**) Entire BOLD time series in the three analyzed regions. During the first and last stimulation block (low-intensity stimulation trains), no stimulus-related variation in BOLD signal intensities was observed, whereas during the second stimulation block (high-intensity stimulation trains), each stimulus train caused a clear BOLD response in all three regions. However, in the right CA3 region the first high-intensity stimulation train caused a prolonged elevation of BOLD signal intensities so that the BOLD response to the second high-intensity stimulation train was not clearly detectable.

a widely distributed BOLD response in the left, stimulated hippocampus and a more focused BOLD response in the right hippocampus (Figure 3A). This wide distribution of significant BOLD responses in the left hippocampus confirms the presence of a large number of associational fibers projecting to the whole transverse extent of the CA3b, and to all CA3 pyramidal cells in the septal direction (CA3a) within the CA3 associational pathway.[15] The HRF to individual stimulation trains was similar in the left and right hippocampus, but different in the septum. A smaller magnitude and a slower raising slope characterized the HRF in the septum, so that the maximal BOLD signal intensity was delayed by 1.4 seconds when compared with the hippocampus (Figure 3B, Table 1).

The BOLD responses in the right hippocampus to individual stimulation trains varied; the first stimulation train triggered the strongest BOLD response, and all subsequent stimulation trains generated smaller BOLD responses (Figures 3C and 6). The variations of the BOLD responses moderately correlated with variations in the average slopes of the fEPSP ($R^2 = 0.5202$, $t_{(df:\ 8)} = -2.9454$, $P = 0.0185$) and with the average latencies of the fEPSPs ($R^2 = 0.6013$, $t_{(df:\ 8)} = -3.4739$, $P = 0.007$; Figure 6).

Correlation of the Blood Oxygen Level-Dependent Response and Pyramidal Cell Activity in the Right CA1 Region during Electrical Stimulation of the Left CA3c Region

Electrical stimulation of the left CA3c with low-intensity pulses also caused substantial postsynaptic activations in the right CA1 region. Similar to repetitive stimulations of the left CA3a/b region, the fEPSPs did not change during consecutive pulses within each stimulus train and during consecutive trains. Again, these postsynaptic activations did not cause significant changes in BOLD signal intensities. Increasing the stimulation intensity triggered significantly stronger postsynaptic activations in the right CA1 region that coincided with substantial spiking of the CA1 pyramidal cells as detected by the clear population spike component (Figures 1 and 4A). Within all stimulation trains the slopes of fEPSPs declined, whereas the corresponding latencies increased (Figure 5). In contrast to the postsynaptic responses, spiking—as measured as amplitude of the population spike component—gradually increased in each stimulus train; thus, a facilitation of the spiking activity occurred during each train. The corresponding population spike latencies increased only after the first pulse and then remained on this elevated level (Figure 5).

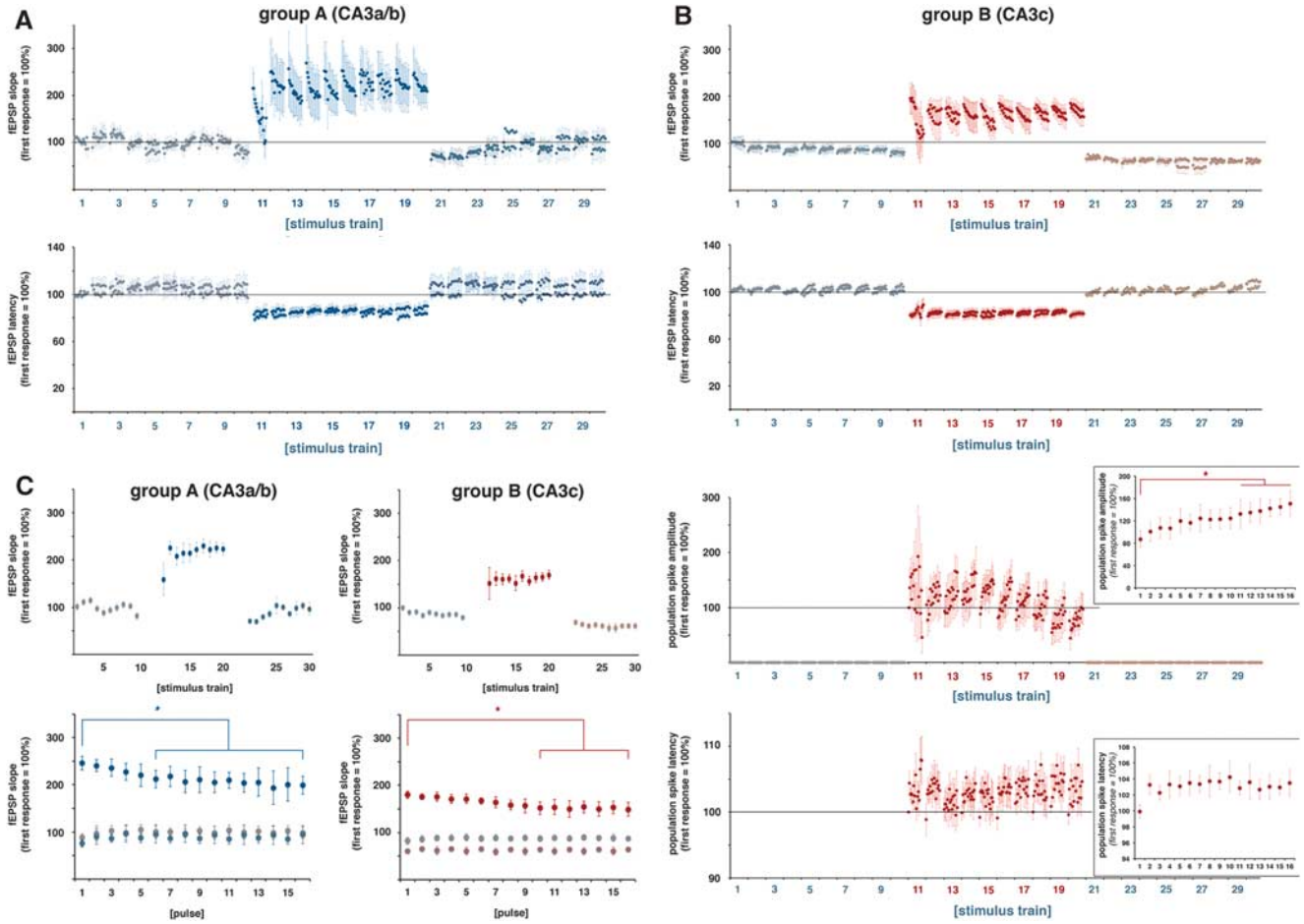

Figure 5. Consecutively applied pulses within one stimulation train and between consecutive stimulation trains caused variations in the electrophysiologic responses of the right CA1 pyramidal cells. (**A**) Development of the field excitatory postsynaptic potential (fEPSP) slopes and latencies in the right CA1 region during repetitive electrical stimulation of the left CA3a/b region with low-intensity (trains 1 to 10), high-intensity (trains 1 to 20), and again low-intensity stimulation trains (trains 21 to 30). During each train, 16 responses were recorded. The response to the first low-intensity stimulation pulse in train 1 was set to 100% ($n = 6$). (**B**) Development of the fEPSP slopes and latencies and population spike amplitudes and latencies in the right CA1 region during repetitive electrical stimulation of the left CA3c region with low-intensity (trains 1 to 10), high-intensity (trains 1 to 20), and again low-intensity stimulation trains (trains 21 to 30). The fEPSP response to the first low-intensity stimulation pulse in train 1 was set to 100% and the population spike response to the first high-intensity pulse was set to 100% ($n = 6$). The inserts represent the average development of the population spike amplitudes and latencies during the high-intensity stimulation trains ($n = 6$, significant change to the first response is indicated by an asterisk (paired Student's *t*-test, df: 5). (**C**) Upper row: Plot of the averaged responses to all 16 pulses per train to depict variations in neuronal activity during consecutive trains. Lower row: Plot of the average responses to consecutive pulses during the initial low-intensity trains (i.e, trains 1 to 10; gray dots), the high-intensity stimulation trains (i.e., trains 11 to 20, dark blue dots (group A) or dark red dots (group B)) and the following low-intensity stimulation trains (i.e., trains 21 to 30; gray blue (group A) or gray red (group B)). Asterisks show significant lower responses in comparison with the corresponding first pulse during the high-intensity stimulation train (paired Student's *t*-test, $n = 6$, df: 5).

During consecutive stimulation trains, the average postsynaptic activations remained similar, i.e., no significant changes in the average slope and latency of the fEPSP were observed. In contrast, the average population spike amplitude decreased and the average population spike latency decreased after the first train and recovered to almost the initial level during all subsequent trains (Figure 6).

The high-intensity stimulation of the left CA3c region also triggered significant BOLD responses in the left and right hippocampus, as well as in the septal region (Figure 4A). However, in contrast to electrical stimulation of the left CA3a/b region, stimulation of the left CA3c region only resulted in a sparse distribution of significant BOLD responses in the left hippocampus, whereas the spatial distribution in the right hippocampus and septal area was similar. This sparse distribution of significant BOLD responses in the left hippocampus confirms the known limited local projection of the CA3c neurons within the CA3 associational pathway.[15]

The BOLD responses in the right CA1 region during consecutive high-intensity stimulation trains varied (Figures 4C and 5). Correlation of the generated BOLD response with concurrent measured parameters of postsynaptic activity (fEPSP slope: $R^2 = 0.1286$, $t_{(df:\ 8)} = -1.0867$, $P = 0.3088$, fEPSP latency: $R^2 = 0.0636$, $t_{(df:\ 8)} = 0.7371$, $P = 0.4821$) and spiking activity (population spike amplitude: $R^2 = 0.0401$, $t_{(df:\ 8)} = -0.5782$, $P = 0.5790$, population spike latency $R^2 = 0.1397$, $t_{(df:\ 8)} = 1.1400$, $P = 0.2873$) revealed no significant relation between the activity of the principal cells and the resultant BOLD response (Figure 6).

DISCUSSION

The current study aimed to determine the specific role of postsynaptic activity of principal neurons for the resultant BOLD response in the rat CA1 region. By using two related stimulation protocols, i.e., stimulating either the left CA3a/b or CA3c region,

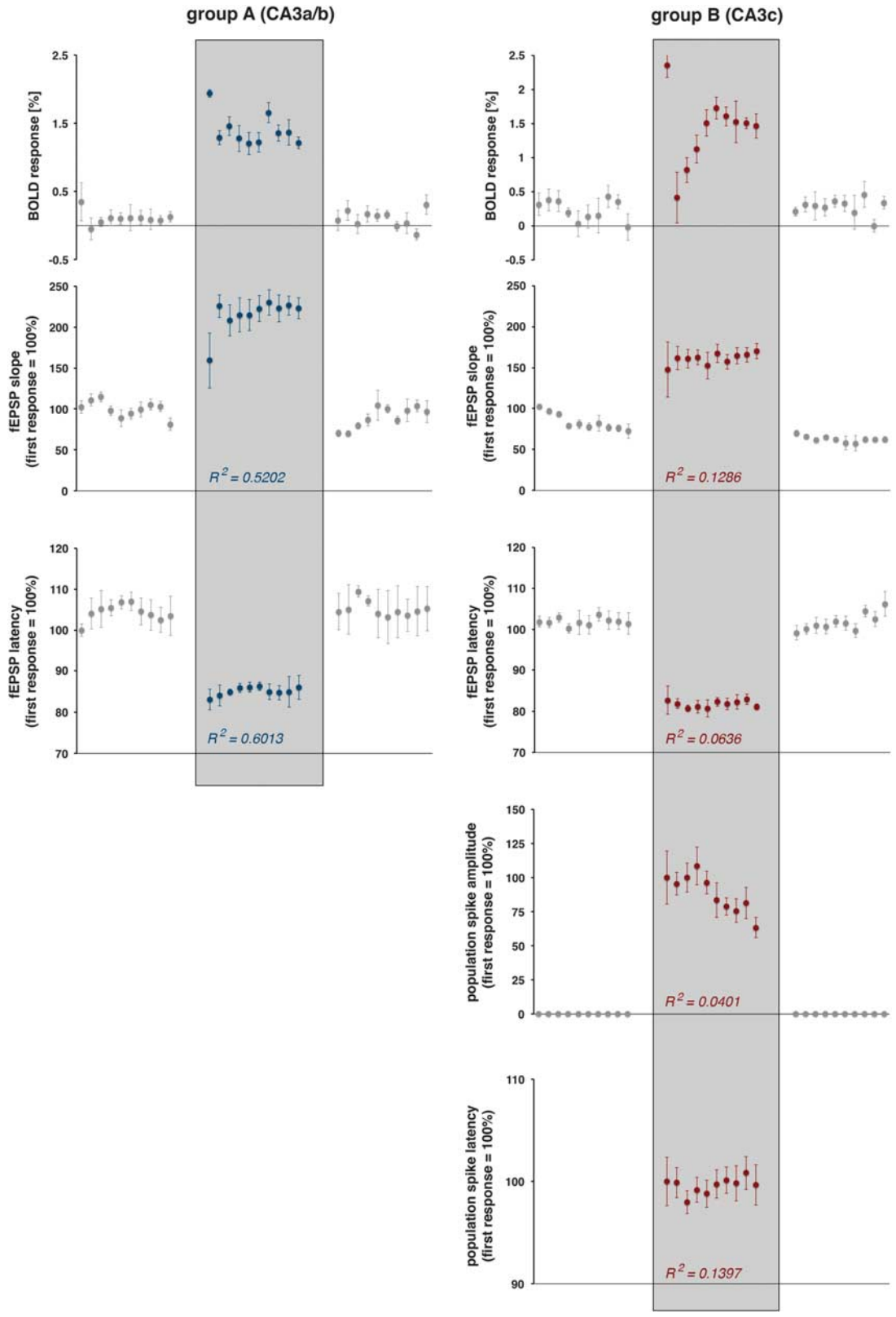

Figure 6. Development of blood oxygen level-dependent (BOLD) responses and simultaneously measured electrophysiologic responses during consecutive stimulation trains. The magnitude of the BOLD response and the concurrently measured average values of electrophysiologically measured parameters of neuronal activity are shown The Pearson correlation coefficient (R^2) indicates the relation between the electrophysiologically measured parameter and the resultant BOLD response high-intensity stimulation trains (sample size 10; df: 8).

Table 1. Summary of the measured maximal BOLD responses during consecutive high-intensity stimulation trains (corrected BOLD values)

	Electrical stimulation of the left CA3a/b (group A)		*Electrical stimulation of the left CA3c (group B)*		P
	$BOLD_{max}$	t_{max}	$BOLD_{max}$	t_{max}	
Right HC					
Trains 1–10	1.42 ± 0.23	7.80 ± 0.63	1.41 ± 0.53	7.80 ± 1.48	
Train 1	1.94	8.00	2.36	10.00	
Trains 1–5	1.43 ± 0.30	8.00 ± 0.00	1.24 ± 0.74	8.40 ± 1.67	
Trains 6–10	1.36 ± 0.18	7.20 ± 1.10	1.56 ± 0.10	7.20 ± 1.1	
Volume	129 ± 18		128 ± 47		
Left HC					
Trains 1–10	1.69 ± 0.24	7.60 ± 0.84	1.32 ± 0.31	8.00 ± 0.00	< 0.01
Train 1	2.18	8.00	1.91	8.00	
Trains 1–5	1.60 ± 0.31	8.0 ± 0.00	1.22 ± 0.42	8.00 ± 0.00	
Trains 6–10	1.80 ± 0.09	7.20 ± 1.10	1.42 ± 0.11	8.00 ± 0.00	< 0.001
Volume	188 ± 33		43 ± 11		0.01
Septum					
Trains 1–10	1.03 ± 0.18	9.20 ± 1.03	0.86 ± 0.24	9.40 ± 1.35	
Train 1	1.06	8.00	1.09	12.00	
Trains 1–5	1.03 ± 0.21	9.60 ± 1.67	0.69 ± 0.18	8.80 ± 1.10	< 0.05
Trains 6–10	1.02 ± 0.16	10.0 ± 2.00	1.02 ± 0.19	10.00 ± 1.41	
Volume	18 ± 6		10 ± 5		

BOLD, blood oxygen level-dependent; HC, hippocampus. The volume represents the number of significantly activated voxels ($t_{min} = 4$) in the region of interest. *P* values (Student's *t*-test, df:10) for significant differences in the maximal BOLD response between the two groups are listed right.

the postsynaptic activity was, on the one hand, associated with strong spiking, and on the other hand, only associated with minor spiking of the principal cells.

The main results of the present study are as follows: (1) substantial postsynaptic activity of principal cells without spiking do not necessarily generate significant BOLD responses; (2) repetitive identical electrical stimulations of the left CA3 cause variations in postsynaptic responses of pyramidal cells in the right CA1 region, which were also accompanied with variations in the resultant BOLD responses; (3) parameters of postsynaptic activity of pyramidal cells, such as slope and latency of the fEPSP, did not positively correlate with the concurrent generated BOLD response; and (4) additional strong spiking of CA1 pyramidal cells causes a greater variability in the triggered BOLD response, but spiking activity of the pyramidal cells did not correlate with the magnitude of the BOLD response.

Synaptic activity, meanwhile, is generally assumed to be the main factor controlling the magnitude of a BOLD response. In a seminal study, Logothetis *et al*[5] could show that in the visual cortex, stimulus-induced local field potentials rather than multi-unit activity correlate with concurrently measured BOLD responses. Because the measured local field potential is more closely related to synaptic than spiking activity, this conclusion is coherent. However, not only do synaptic activity affect the measured local field potential, but also Ca^{2+} spikes, voltage-dependent intrinsic events, action potentials, and spike after-potentials.[20] Consequently, all of these factors may substantially contribute to the measured BOLD signal. Later studies indicate that the amount of principal cell spiking does not relate, and therefore predicts the magnitude of a BOLD response. Significant BOLD responses can be generated even without any spiking of the principle cells,[21] which is in line with a previous laser Doppler flow technique study that already indicated that synaptic activity (but not spiking activity) of principal cells controls the vascular response in the cerebellum.[22] However, assigning synaptic activity as the main determinant for the generated BOLD response still does not clearly attribute what part of the synaptic process primarily controls the neurovascular coupling mechanism. In general, there are two conceivable, independently acting mechanisms. First, the presynaptically released transmitter and putative co-released vasoactive factors control the hemodynamic response either directly or through activated glia cells, which tightly surround the synapses. Second, postsynaptic depolarizations and the ensuing energy-demanding repolarizations and (glia-mediated) transmitter recycling control the blood supply in this region. Although the first mechanism can be regarded as feedforward control, the second scenario refers to a feedback control for the neurovascular coupling.[2]

In the hippocampal CA1 region, pyramidal neurons are by far the most numerous neurons.[23] Interneurons account for only 7%[24] to 11%[25] of all neurons. Thus, the synchronized activity of the principal neurons should have a significant effect on the generated BOLD responses, at least as soon as their summed neuronal activity determines the magnitude of the BOLD response. Evidently, this was not the case. The development of the summed postsynaptic responses and, if present, the spiking of the CA1 pyramidal neurons to repetitive stimulation trains did not match the development of concurrently generated BOLD responses. Consequently, a simple metabolic-mediated feedback control of vascular systems resulting from an increased energy demand of the activated pyramidal neurons appears, at least in the CA1 region, very unlikely. This implies that under the used experimental circumstances, the activity of the principal cells may still contribute to the fMRI response, but this activity is not pivotal for the measured size of the BOLD response. Therefore, other factors control the magnitude of the BOLD response. These may include (1) the activity of (inhibitory) interneurons that are also activated during stimulation and (2) stimulus-induced mechanisms upstream of the pyramidal neuron within the CA1 region.

Commissural collaterals projecting to the CA1 region target both pyramidal neurons and (inhibitory) interneurons. Furthermore, once activated, pyramidal neurons target GABAergic basket cells, bistratified cells, and OL-M cells, which in turn mediate a feedback inhibition on the pyramidal neurons.[26]

A stimulus-dependent increase in the activity of these GABAergic interneurons should have a detectable inhibitory effect on principal neurons, the pyramidal neurons. During the high-intensity pulse stimulation protocol (i.e., trains 11 to 20), the synaptic responses to the 16 consecutive pulses significantly decreased (Figure 5). However, whether the decline in postsynaptic responses of the pyramidal cells relates to variations in the presynaptic transmitter release or to an increased activity of inhibitory synapses cannot be addressed by the used experimental approach. At the same time, the population spike amplitude increased, thus during consecutive high-intensity pulses the excitatory postsynaptic potential-spike coupling (E-S coupling) enhanced. This coincides with the generation of a significant BOLD response. The observation that under this condition the size of the BOLD response did not correlate with the spiking or postsynaptic activity of the pyramidal cells supports previous findings,[7] indicating that in the presence of an increased intrinsic excitability of the principal neurons mainly signaling cascades upstream of the principal cells determine the BOLD response.

In contrast, during the low-intensity stimulation protocol (i.e., trains 1 to 10 and 21 to 30) the synaptic responses to consecutive pulses did not decline, indicating that no inhibitory components were activated. Even though the slope of the fEPSP increased during consecutive low-intensity stimulation pulses no population spikes were generated. Consequently, possible changes in the intrinsic excitability of the pyramidal cells cannot be determined. However, under this condition no significant changes in BOLD signal intensities were observed.

It appears that mechanisms upstream of the principal cells that become activated by the incoming stimuli control the magnitude of the BOLD response. This may include glia cells, which may become directly activated by the presynaptically released glutamate or may become metabolically active as a result of glutamate uptake and glutamate-glutamine cycling.[2] Activated glia cells may in turn release various vasoactive substances, such as arachidonic acid metabolites (e.g., prostaglandin E_2), epoxyeicosatrienoic acid, and D-serine,[27–30] and control by that vascular response.

In the current study, the strength of presynaptic activity in the right CA1 region was not studied, nor were any putative variations in presynaptic transmitter release during consecutive stimulations. Therefore, the authors can only speculate about the specific role of presynaptic activity for the generation of a BOLD response. However, as long as the postsynaptic and spiking activity of the most abundant neurons do not directly control the vascular response, other mechanism(s) that are activated by the presynaptically released transmitter and cofactors become(s) crucial for mediating the neurovascular coupling. No BOLD response was observed during sole presynaptic/postsynaptic activations, i.e., during application of consecutive low-intensity pulses. This may indicate that the amount of input activity in the CA1 region is not sufficient enough to modify the vascular response, or that input-related mechanisms can affect only the vascular response when concurrent principal cells and/or interneurons in the CA1 regions generate action potentials and process by that the incoming signals. The second assumption would support previous findings that the neurovascular coupling consists of at least two different mechanisms, namely, a presynaptically and a spiking-controlled component, whereupon the actual contribution depends on the current intrinsic excitability of the principal neurons.[7]

In conclusion, direct evidence was presented that postsynaptic and spiking activity of CA1 pyramidal cells, the most abundant neurons in this region, do not control the magnitude of the BOLD response in the rat CA1 region. For that, a new experimental approach was used to measure simultaneously the summed postsynaptic activity of pyramidal cells in the rat CA1 region and the concurrently generated BOLD response during electrical stimulation of contralateral CA3 neurons that monosynaptically project to the CA1 region. Furthermore, more indirect evidence exclude a pivotal role of the local interneurons in the formation of a BOLD response. All of those results indicate that the magnitude of the BOLD response is not linearly related to the postsynaptic activity of local principal and interneurons. However, for eventually forming a stimulus-related BOLD response, a strong postsynaptic activity, sufficient to generate action potentials, appears to be necessary. Consequently, the postsynaptic activity of principal neurons is not the main predictor for the magnitude of formed BOLD responses in the hippocampal CA1 region.

DISCLOSURE/CONFLICT OF INTEREST

The authors declare no conflict of interest.

ACKNOWLEDGMENTS

The authors wish to thank Jeanette Maiwald for her excellent technical assistance in the histological verification of the electrode locations.

REFERENCES

1 Ogawa S, Lee TM, Kay AR, Tank DW. Brain magnetic resonance imaging with contrast dependent on blood oxygenation. *Proc Natl Acad Sci USA* 1990; **87**: 9868–9872.
2 Attwell D, Buchan AM, Charpak S, Lauritzen M, Macvicar BA, Newman EA. Glial and neuronal control of brain blood flow. *Nature* 2010; **468**: 232–243.
3 Attwell D, Iadecola C. The neural basis of functional brain imaging signals. *Trends Neurosci* 2002; **25**: 621–625.
4 Donahue MJ, Near J, Blicher JU, Jezzard P. Baseline GABA concentration and fMRI response. *Neuroimage* 2010; **53**: 392–398.
5 Logothetis NK, Pauls J, Augath M, Trinath T, Oeltermann A. Neurophysiological investigation of the basis of the fMRI signal. *Nature* 2001; **412**: 150–157.
6 Mukamel R, Gelbard H, Arieli A, Hasson U, Fried I, Malach R. Coupling between neuronal firing, field potentials, and FMRI in human auditory cortex. *Science* 2005; **309**: 951–954.
7 Angenstein F. The actual intrinsic excitability of granular cells determines the ruling neurovascular coupling mechanism in the rat dentate gyrus. *J Neurosci* 2014; ;**34**: 8529–8545.
8 Angenstein F, Kammerer E, Niessen HG, Frey JU, Scheich H, Frey S. Frequency-dependent activation pattern in the rat hippocampus, a simultaneous electrophysiological and fMRI study. *Neuroimage* 2007; **38**: 150–163.
9 Kaibara T, Leung LS. Basal versus apical dendritic long-term potentiation of commissural afferents to hippocampal CA1: a current-source density study. *J Neurosci* 1993; **13**: 2391–2404.
10 Scherf T, Frey JU, Frey S. Simultaneous recording of the field-EPSP as well as the population spike in the CA1 region in freely moving rats by using a fixed "double"-recording electrode. *J Neurosci Methods* 2010; **188**: 1–6.
11 Schwartzkroin PA. Characteristics of CA1 neurons recorded intracellularly in the hippocampal in vitro slice preparation. *Brain Res* 1975; **85**: 423–436.
12 Andersen P, Silfvenius H, Sundberg SH, Sveen O. A comparison of distal and proximal dendritic synapses on CAi pyramids in guinea-pig hippocampal slices in vitro. *J Physiol* 1980; **307**: 273–299.
13 Andersen P, Morris R, Amaral D, Bliss T, O'Keefe J. Field potential analysis. *The hippocampus book*. Oxford University Press: Oxford, New York , 2007; 27–30.
14 Lorente de Nó R. Studies on the structure of the cerebral cortex II. Continuation of the study of the ammonic system. *J Psychol Neurol* 1934; **46**: 113–117.
15 Bernard C, Wheal HV. Model of local connectivity patterns in CA3 and CA1 areas of the hippocampus. *Hippocampus* 1994; **4**: 497–529.
16 Li XG. The hippocampal CA3 network: An in vivo intracellular labeleling study. *J Comp Neurol* 1994; **339**: 181–208.
17 Paxinos G, Watson C. *The rat brain in stereotaxic coordinates*. Academic Press: San Diego, 1988.
18 Weber R, Ramos-Cabrer P, Wiedermann D, van Camp N, Hoehn M. A fully non-invasive and robust experimental protocol for longitudinal fMRI studies in the rat. *Neuroimage* 2006; **29**: 1303–1310.
19 Hennig J, Nauerth A, Friedburg H. RARE imaging: a fast imaging method for clinical MR. *Magn Reson Med* 1986; **3**: 823–833.
20 Buzsaki G, Anastassiou CA, Koch C. The origin of extracellular fields and currents--EEG, ECoG, LFP and spikes. *Nat Rev Neurosci* 2012; **13**: 407–420.
21 Angenstein F, Krautwald K, Scheich H. The current functional state of local neuronal circuits controls the magnitude of a BOLD response to incoming stimuli. *Neuroimage* 2010; **50**: 1364–1375.

22 Mathiesen C, Caesar K, Akgoren N, Lauritzen M. Modification of activity-dependent increases of cerebral blood flow by excitatory synaptic activity and spikes in rat cerebellar cortex. *J Physiol* 1998; **512**, Pt 2 555–566.
23 Amaral D, Lavenex P. Hippocampal neuroanatomy. In: Andersen P, Morris R, Amaral D, Bliss T, O'Keefe J (eds) *The hippocampus book*. Oxford University Press: Oxford, New York, 2007 pp 37–114.
24 Aika Y, Ren JQ, Kosaka K, Kosaka T. Quantitative analysis of GABA-like-immunoreactive and parvalbumin-containing neurons in the CA1 region of the rat hippocampus using a stereological method, the disector. *Exp Brain Res* 1994; **99**: 267–276.
25 Woodson W, Nitecka L, Ben-Ari Y. Organization of the GABAergic system in the rat hippocampal formation: a quantitative immunocytochemical study. *J Comp Neurol* 1989; **280**: 254–271.
26 Buhl E, Whittington M. Local circuits. In: Andersen P, Morris R, Amaral D, Bliss T, O'Keefe J (eds) *The hippocampus book*. Oxford University Press: Oxford, New York, 2007 pp 297–319.
27 Koehler RC, Roman RJ, Harder DR. Astrocytes and the regulation of cerebral blood flow. *Trends Neurosci* 2009; **32**: 160–169.
28 Park J, Takmakov P, Wightman RM. In vivo comparison of norepinephrine and dopamine release in rat brain by simultaneous measurements with fast-scan cyclic voltammetry. *J Neurochem* 2011; **119**: 932–944.
29 Petzold GC, Murthy VN. Role of astrocytes in neurovascular coupling. *Neuron* 2011; **71**: 782–797.
30 Stobart JL, Lu L, Anderson HD, Mori H, Anderson CM. Astrocyte-induced cortical vasodilation is mediated by D-serine and endothelial nitric oxide synthase. *Proc Natl Acad Sci USA* 2013; **110**: 3149–3154.